

Radiation dosimetry of ^{68}Ga -PSMA-11 (HBED-CC) and preliminary evaluation of optimal imaging timing

Ali Afshar-Oromieh^{1,2} · Henrik Hetzheim³ · Wolfgang Kübler⁴ · Clemens Kratochwil¹ · Frederik L. Giesel¹ · Thomas A. Hope⁵ · Matthias Eder⁶ · Michael Eisenhut⁶ · Klaus Kopka⁶ · Uwe Haberkorn^{1,2}

Received: 7 March 2016 / Accepted: 9 May 2016 / Published online: 3 June 2016
© Springer-Verlag Berlin Heidelberg 2016

Abstract

Purpose The clinical introduction of ^{68}Ga -PSMA-11 (“HBED-CC”) ligand targeting the prostate-specific membrane antigen (PSMA) has been regarded as a significant step forward in the diagnosis of prostate cancer (PCa). In this study, we provide human dosimetry and data on optimal timing of PET imaging after injection.

Methods Four patients with recurrent PCa were referred for ^{68}Ga -PSMA-11 PET/CT. Whole-body PET/CT_{low-dose} scans were conducted at 5 min, and 1, 2, 3, 4 and 5 h after injection of 152–198 MBq ^{68}Ga -PSMA-11. Organs of moderate to high uptake were used as source organs; their total activity was determined at all measured time points. Time–activity curves were created for each source organ as well as for the

remainder. The radiation exposure of a ^{68}Ga -PSMA-11 PET was identified using the OLINDA-EXM software. In addition, tracer uptake was measured in 16 sites of metastases.

Results The highest tracer uptake was observed in the kidneys, liver, upper large intestine, and the urinary bladder. Mean organ doses were: kidneys 0.262 ± 0.098 mGy/MBq, liver 0.031 ± 0.004 mGy/MBq, upper large intestine 0.054 ± 0.041 mGy/MBq, urinary bladder 0.13 ± 0.059 mGy/MBq. The calculated mean effective dose was 0.023 ± 0.004 mSv/MBq ($=0.085 \pm 0.015$ rem/mCi). Most tumor lesions ($n=16$) were visible at 3 h p.i., while at all other time points many were not qualitatively present (10/16 visible at 1 h p.i.).

Conclusions The mean effective dose of a ^{68}Ga -PSMA-11 PET is 0.023 mSv/MBq. A 3-h delay after injection was optimal timing for ^{68}Ga -PSMA-11 PET/CT in this patient cohort.

Electronic supplementary material The online version of this article (doi:10.1007/s00259-016-3419-0) contains supplementary material, which is available to authorized users.

Keywords Prostate cancer · PET/CT · HBED-CC · PSMA-11 · Prostate-specific membrane antigen · Dosimetry

✉ Ali Afshar-Oromieh
a.afshar@gmx.de

Introduction

Prostate cancer (PCa) is the most frequent malignant tumor in men worldwide [1]. The diagnosis of recurrent PCa has always been challenging for conventional imaging modalities such as computer tomography (CT) and magnetic resonance imaging (MRI) due to low sensitivity and specificity. Although positron emission tomography (PET) with choline has been regarded as one of the best methods for imaging recurrent PCa, numerous studies reported a low sensitivity and specificity, especially at low prostate specific antigen (PSA) levels and high Gleason scores (GSC) [2–5].

Due to these experiences, the development of improved imaging methods was required. In this context, prostate-

- ¹ Department of Nuclear Medicine, Heidelberg University Hospital, INF 400, 69120 Heidelberg, Germany
- ² Clinical Cooperation Unit Nuclear Medicine, German Cancer Research Center, INF 280, 69120 Heidelberg, Germany
- ³ Division of Medical Physics in Radiology, German Cancer Research Center, INF 280, 69120 Heidelberg, Germany
- ⁴ Division of Radiation Protection and Dosimetry, German Cancer Research Center, INF 280, 69120 Heidelberg, Germany
- ⁵ Department of Radiology and Biomedical Imaging, University of California, 505 Parnassus Avenue, M-391, Box 0628, San Francisco, CA 94143, USA
- ⁶ Division of Radiopharmaceutical Chemistry, German Cancer Research Center, INF 280, 69120 Heidelberg, Germany

Table 1 Characteristics of the patients investigated in this evaluation

Patient no.	Age (years)	⁶⁸ Ga-PSMA-11 (MBq)	GSC	PSA (ng/ml)	Previous treatment	LN metast.	Bone metast.	Local relapse	Soft tissue metast.	Primary tumor
1	62	152	7	1.90	RT	0	0	0	0	0
2	67	170	7	1.49	RPx + RT	4	0	0	0	0
3	72	198	8	4.50	RT	5	0	0	0	0
4	70	173	9	2.10	RT	2	5	0	0	0

RPx radical prostatectomy, RT radiation therapy

specific membrane antigen (PSMA) targeted imaging has received increased attention during the past few years. PSMA is a cell-surface protein that is strongly overexpressed in PCa cells compared to other PSMA-expressing tissues such as salivary glands, liver, kidneys, or intestines [6, 7]. Therefore, it provides a promising target for molecular imaging and therapy of PCa. During the last two decades, many efforts have been undertaken to develop PSMA-ligands [8–15]. In 2011, the low-molecular-weight PSMA-inhibitor Glu-NH-CO-NH-Lys-(Ahx)-[⁶⁸Ga(HBED-CC)] (⁶⁸Ga-PSMA-11) was introduced to the community as a novel PET-tracer for diagnosing PCa [16, 17]. PSMA-11 is also known as PSMA^{HBED}, Glu-CO-Lys(Ahx)-HBED-CC, DKFZ-PSMA-11, PSMA-HBED-CC, PSMA-HBED, or PSMA.

Since the first human ⁶⁸Ga-PSMA-11 PET/CT in May 2011, this novel method of imaging has rapidly spread to multiple institutions [18–20]. These first results were recently confirmed by larger studies [21, 22]. Despite the extensive use of the agent, human dosimetry data as well as an overview about the best time to conduct PET-images after injection of the tracer have not yet been published. The aim of this manuscript was to evaluate such data to close this gap.

Materials and methods

For this evaluation, we performed a retrospective analysis of four patients (Table 1) who underwent ⁶⁸Ga-PSMA-11 PET/CT to detect tumor lesions in case of biochemical relapse of PCa. The mean age of the patients was 68±4 years (range, 62–72 years) with a median GSC of 8 (range, 7–9). The mean PSA level was 2.50±1.36 ng/ml (range, 1.49–4.50 ng/ml). Given patient approval, six PET scans were conducted in order to maximize the chance of detecting tumor lesions and to optimize the tumor staging of the patients.

All patients included in this manuscript signed a written informed consent form allowing anonymized evaluation and publication of their data. This study was in accordance with the Helsinki Declaration and with our national regulations (German Medicinal Products Act, AMG §13 2b). This

evaluation was approved by the ethics committee of the University of Heidelberg.

Radiotracer

The radiotracer was produced as published before [16, 17, 23]: ⁶⁸Ga³⁺ was obtained from a ⁶⁸Ge/⁶⁸Ga radionuclide generator (iThemba IDB-Holland bv, Baarle-Nassau, The Netherlands) and used for radiolabeling of PSMA-11.



Fig. 1 Maximum intensity projection (MIP) of patient one with normal distribution of ⁶⁸Ga-PSMA-11 1 h p.i. Accumulation is seen in lacrimal and salivary glands, nasal mucosa, liver, spleen, proximal small intestines, parts of the colon and in the kidneys. ⁶⁸Ga-PSMA-11 is mainly excreted via the urinary tract

Table 2 Dosimetry data, time-integrated activity coefficient of ⁶⁸Ga-PSMA-11

Patient →	1	2	3	4	Mean (± SD)
	Time integrated activity coefficient [Bq*h/Bq]				
Liver	0.1080	0.0918	0.0847	0.1190	0.1009 (±0.0155)
Spleen	0.0083	0.0199	0.0088	0.0244	0.0154 (±0.0080)
Kidneys	0.0747	0.1790	0.1970	0.2200	0.1677 (±0.0642)
Urinary bladder	0.0965	0.1200	0.1360	0.0672	0.1049 (±0.0299)
Small intestine	0.0059	0.0096	0.0045	0.0039	0.0060 (±0.0026)
Colon	0.0166	0.1070	0.0283	0.0237	0.0439 (±0.0423)
Remainder	1.2100	1.0300	1.0500	1.1200	1.1025 (±0.0814)

The final product was formulated in isotonic PBS and was sterile filtered. The radiolabeling and purification of the PSMA ligand was performed with an automated radio synthesizer [23]. Typically, radiochemical yields of 80 % ± 5 % (decay corrected) and radiochemical purity >99 % were achieved. The targeted activity of ⁶⁸Ga-PSMA-11 was 2 MBq per kg body weight. Variation of injected radiotracer activity between patients was caused by the short physical half-life of ⁶⁸Ga (68 min) and variable elution efficiencies resulting during

the lifetime of the ⁶⁸Ge/⁶⁸Ga generator. All injections contained less than 0.6 µg/ml PSMA-11.

Imaging

The patients were imaged on a BIOGRAPH-mCT PET/CT (Siemens, Erlangen, Germany) after intravenous bolus injection (mean, 173 ± 19 MBq, range, 152–198 MBq). A non-contrast-enhanced CT scan was performed at 5 min, and 1, 2, 3, 4, and 5 h post tracer injection using the following parameters: slice thickness of 5 mm; increment of 2 mm; soft tissue reconstruction kernel; 120 keV/60 mAs at 3-h post injection (p.i.) and 80 keV/30 mAs at 5 min, and 1, 2, 4, and 5 h p.i. These lower keV and mAs were chosen to reduce the radiation exposure by CT. The lower KeV and mAs used should not affect uptake quantification [24].

Immediately after CT scanning, a whole-body (WB) PET was acquired in 3D (matrix: 200 × 200). Each bed position (axial field of view of 16.2 cm) was acquired for 3 min. The emission data were corrected for decay, random and scatter events. Reconstruction was conducted with an ordered subset expectation maximization algorithm (OSEM) with two iterations/eight subsets and Gauss-filtered to a transaxial

Table 3 Absorbed organ doses of a ⁶⁸Ga-PSMA-11 PET

Patient →	1	2	3	4	Mean (± SD)
	Absorbed Organ Dose (mGy/MBq)				
Adrenals	0.0134	0.0138	0.0139	0.0155	0.0142 (±0.0009)
Brain	0.0098	0.0084	0.0085	0.0091	0.0090 (±0.0007)
Breasts	0.0092	0.0084	0.0085	0.0092	0.0088 (±0.0004)
Gallbladder	0.0141	0.0148	0.0136	0.0150	0.0144 (±0.0006)
Lower colon	0.0128	0.0122	0.0121	0.0119	0.0123 (±0.0004)
Small intestine	0.0159	0.0195	0.0148	0.0149	0.0163 (±0.0022)
Stomach	0.0121	0.0119	0.0114	0.0125	0.0120 (±0.0005)
Upper colon	0.0284	0.1160	0.0391	0.0325	0.0540 (±0.0416)
Heart	0.0117	0.0103	0.0104	0.0113	0.0109 (±0.0007)
Kidneys	0.1190	0.2790	0.3060	0.3420	0.2620 (±0.0984)
Liver	0.0322	0.0287	0.0265	0.0361	0.0309 (±0.0042)
Lungs	0.0109	0.0096	0.0097	0.0105	0.0102 (±0.0006)
Muscle	0.0110	0.0101	0.0101	0.0106	0.0105 (±0.0004)
Pancreas	0.0133	0.0136	0.0133	0.0149	0.0138 (±0.0008)
Red marrow	0.0094	0.0090	0.0089	0.0094	0.0092 (±0.0003)
Osteogenic cells	0.0153	0.0135	0.0136	0.0145	0.0142 (±0.0008)
Skin	0.0095	0.0084	0.0085	0.0090	0.0085 (±0.0005)
Spleen	0.0255	0.0561	0.0284	0.0682	0.0446 (±0.0209)
Testes	0.0112	0.0099	0.0102	0.0102	0.0104 (±0.0006)
Thymus	0.0108	0.0093	0.0094	0.0101	0.0099 (±0.0007)
Thyroid	0.0106	0.0091	0.0093	0.0099	0.0097 (±0.0007)
Urinary bladder	0.1220	0.1480	0.1660	0.0874	0.1300 (±0.0341)
Total body	0.0123	0.0123	0.0121	0.0130	0.0124 (±0.0004)
Effective dose (mSv/MBq)	0.0183	0.0254	0.0263	0.0242	0.0236 (±0.0036)

resolution of 2 mm at FWHM (full width at half maximum). Attenuation correction was performed using the low-dose non-enhanced CT data acquired at each time point.

Image evaluation

Two board-certified specialists in nuclear medicine with 10 and 27 years of clinical experiences (first and last author) read all data sets independently and resolved any disagreements by consensus.

For calculation of the standardized uptake value (SUV), circular regions of interest were drawn around areas with focally increased uptake in transaxial slices and automatically adapted to a three-dimensional volume of interest at a 70 % isocontour for SUV calculations.

Lesions that were visually considered PCa metastases were counted and analyzed with respect to their localization (local relapses, lymph node, bone, and soft tissue metastases) and to their mean and maximum standardized uptake values (SUVmean and SUVmax) at all time points. Any visible PCa lesions of a patient were counted and analyzed. Tumor contrast

was measured by dividing the SUVmean of tumor lesions by the SUVmean of the background as well as by dividing the SUVmax of tumor lesions by the SUVmax of the background. As background tissue, we selected gluteal musculature.

Radiation dosimetry

The fused PET/CT images were used to define the organs showing moderate and high uptake of ⁶⁸Ga-PSMA-11. The corresponding volume of interests (VOIs) borders were drawn on each WB PET image with the help of PMOD software (PMOD Ltd, Zurich, Switzerland), which were verified visually for adequate placement. The VOIs were defined such that the whole activity of the organ was taken into account and care was taken to minimize interference of adjacent activity distribution in other organs. VOIs were drawn for lacrimal and salivary glands (all of them summed), liver, spleen, both kidneys (summed), proximal small intestines, colon (those parts which took up the tracer, mostly the descendent parts) and urinary bladder. The activity distribution for the four patients was analyzed at 5 min, and 1, 2, 3, 4, and 5 h after intravenous

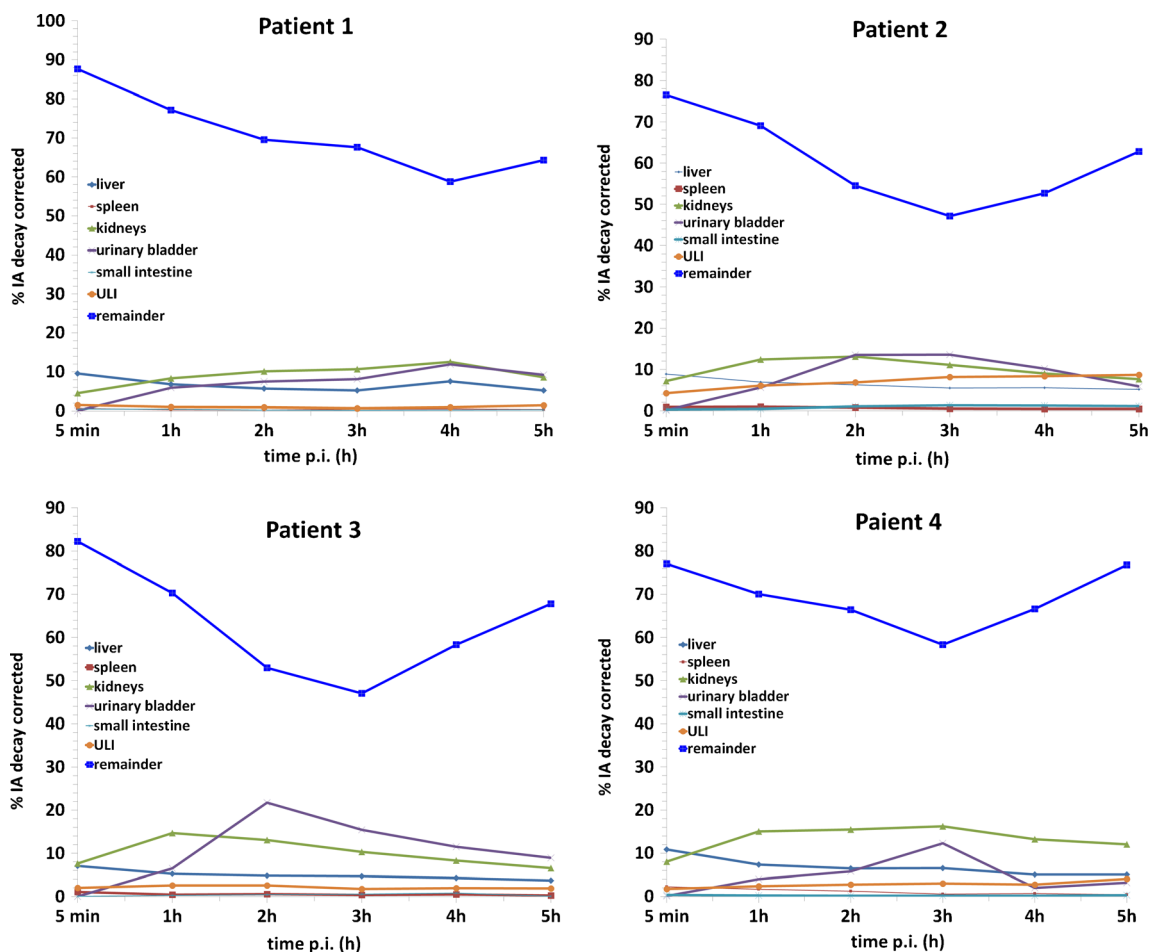


Fig. 2 Organ distribution of ⁶⁸Ga-PSMA-11 of the source organs with the remainder given as a proportion of the injected activity corrected for the physical decay. ULI upper large intestines

injection of ^{68}Ga -PSMA-11 to estimate the absorbed radiation dose. Integration of the time–activity curves for the corresponding organs and tumor sites was used to estimate the time-integrated activity coefficient (Bq*h/Bq) of the tracer in the organs. A bi-exponential fit was used for the integration of the time–activity curves.

The time-integrated activity coefficient of the tracer for each patient was used to calculate the organ dose and the effective dose for the standard 73-kg adult male model with the help of OLINDA/EXM application (version 1.1) [25]. Our specific aim was to estimate the effective dose for a standard patient referred for ^{68}Ga -PSMA-11 PET/CT, not to evaluate the patient-specific dose received. The latter is more important for use with generic patients referred for a PSMA-ligand radiotherapy. We assumed that the fraction of the accumulated activity in the organs was independent from the body mass and we used the standard male model of the OLINDA software. The calculation of the absorbed organ dose and the effective dose was calculated by OLINDA/EXM. The effective dose is based on the recommended weighting factors of the ICRP 60 (1991) report [26].

Additionally, patients were asked to empty their bladder prior to each scan. The activity of the collected excreted urine was then determined separately by measuring a sample of 1 ml twice in a well counter detector (Berthold LB 951G, Bad Wildbad, Germany). The average of the two different measurements was adjusted based on the volume of the collected urine. This urine activity was then added to the calculated urinary bladder content determined from the PET/CT measurement at the same time point. The excreted decay-corrected activity was subtracted from the remainder at the next PET/CT measurement. The remainder is defined as those remaining parts of the body that show low or unspecific tracer uptake.

According to the biodistribution of ^{68}Ga -PSMA-11, it can be assumed that with the exception of lacrimal and salivary glands, liver, spleen, kidneys, urinary bladder, small intestine and colon, the balance of the activity (including the activity within the blood vessels) is uniformly distributed in the remainder. Because ICRP 60 and OLINDA do not provide separate analysis of salivary and lacrimal gland dose, tracer uptake within these glands was contributed to the remainder. This approach has no effect for the estimation of effective dose.

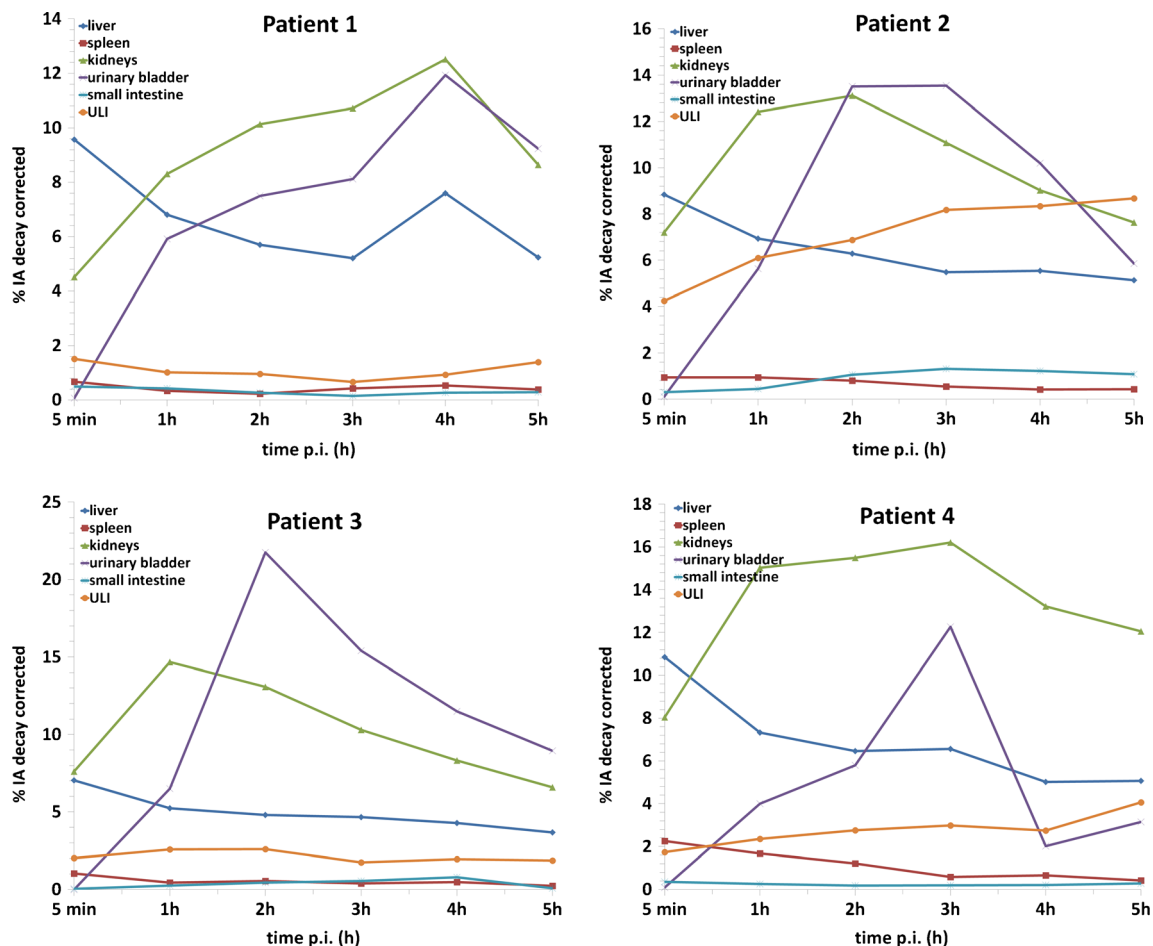


Fig. 3 Organ distribution of ^{68}Ga -PSMA-11 of the source organs without the remainder given as a proportion of the injected activity corrected for the physical decay. *ULI* upper large intestines

Results

None of the patients developed adverse events or clinically detectable pharmacological effects. As presented by Fig. 1, physiological uptake of ^{68}Ga -PSMA-11 was observed in lacrimal and salivary glands, nasal mucosa, liver, spleen, kidneys, proximal small intestines and in some portions of the large intestines. ^{68}Ga -PSMA-11 is excreted via the urinary tracts. In addition, it is known that also celiac ganglia can present with uptake of ^{68}Ga -PSMA-11, especially when using the latest generation of PET scanners [27]. However, none of the patients of the present study showed PSMA-positive celiac ganglia.

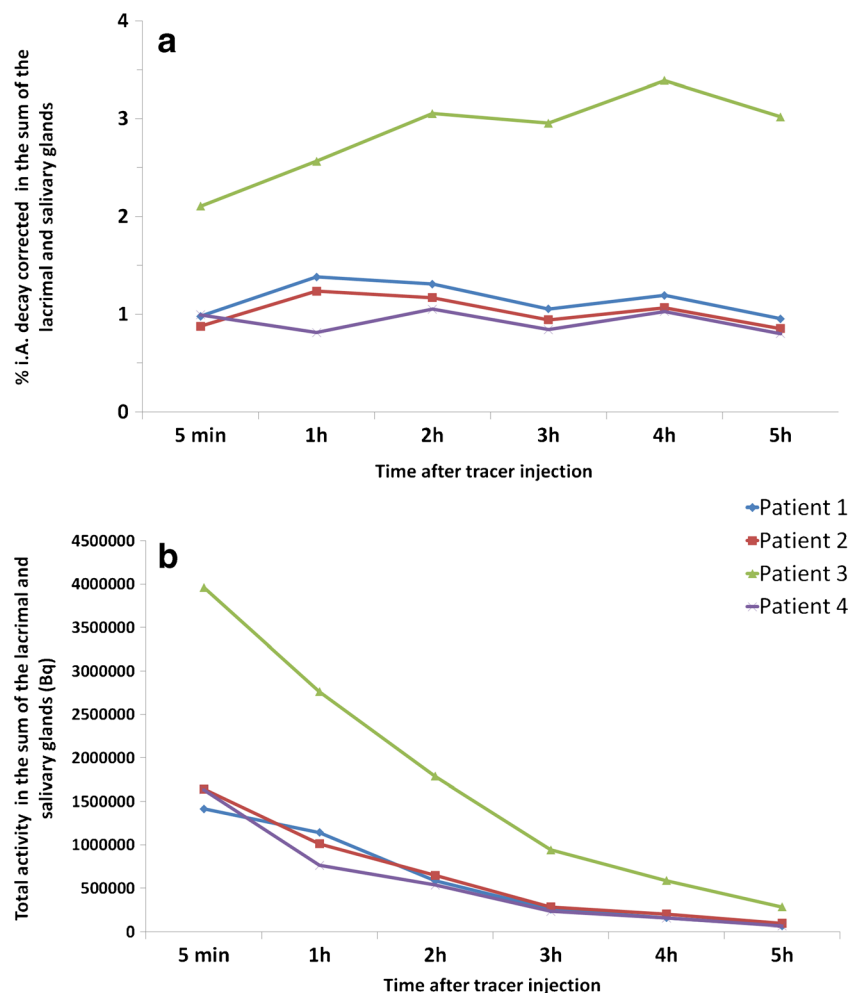
Radiation dosimetry

The effective dose of ^{68}Ga -PSMA-11 was determined in all patients. A mean activity of 173 MBq (152–198 MBq) was injected intravenously. Table 2 provides the estimated time-integrated activity coefficient of ^{68}Ga in the selected source organs. The highest value

occurred for the remainder followed by the kidneys in patients 2–4 and by the liver in patient 1. The estimated organ doses and the effective dose of each patient are shown in Table 3. The mean effective dose per unit activity administered of the four patients was 0.023 ± 0.004 mGy/MBq. The highest organ dose registered in the patient collective was determined in the kidneys of patient 4 with 0.342 mGy/MBq. Looking at the mean value of the absorbed organ doses for the four patients, the three highest dose values were kidneys (0.261 mGy/MBq), the urinary bladder wall (0.130 mGy/MBq) and the upper large intestine wall (0.054 mGy/MBq).

Figures 2 and 3 show the decay-corrected radioactivity in the source organs as a function of time. The remainder activity ranges from 46 to 76 %, whereas the other source organ distributions are in the range of 1–20 %. The activity distribution in the total head (including all lacrimal and salivary glands) was in the range of 1–3 % (Fig. 4). As also demonstrated by Fig. 4, the decay corrected activity in the salivary and lacrimal glands stayed mainly stable by time.

Fig. 4 Decay corrected activity (a) and total activity (b) of the sum of the lacrimal and salivary glands



Evaluation of malignant uptake

Figure 5 presents the uptake and contrast of all metastases in relation to the different times following the injection of ⁶⁸Ga-PSMA-11. The background SUVs are presented by supplementary Table 1. PCa metastases demonstrated an increased uptake and contrast over time (Fig. 6).

Overall, 16 PCa lesions were counted and analyzed in three patients. Eleven were defined as lymph node (LN) metastases (in three patients) and five as bone metastases (in one patient). As demonstrated by Table 4, SUV_{mean} and SUV_{max} increased in most metastases with time. However, not all of the lesions were visible at all scans due to low contrast as also presented by Table 4. The highest detection rate of metastases was at 3 h p.i.

Discussion

Since the introduction of ⁶⁸Ga-PSMA-11 for PET-imaging, PSMA-PET/CT has spread rapidly to many institutions. The whole-body distribution and internal radiation dosimetry of ⁶⁸Ga-PSMA-11 is presented in four patients. The kidneys were the organs receiving the highest absorbed dose (average dose: 0.262 mGy/MBq). Additional organs with higher mean dose were the urinary bladder, upper large intestines and the spleen. The average effective dose with a diagnostic activity

of 200 MBq was 4.7 mSv. These results are similar compared to other most recently introduced PSMA ligands [15, 28].

Patient number 1, in whom no tumor lesion was found, presented with slightly less radiation exposure. One reason could be the fact that in the first 3 h a slower decrease of the activity of the remainder and a slower increase of the activity in the kidneys was observed in this patient. This results in a lower kidney dose and a lower effective dose. The lack of PSMA-positive lesions in this patient is most likely coincidental and unrelated to the lower radiation exposure.

In our analysis, salivary and lacrimal glands were found to have no significant impact on the radiation exposure caused by a ⁶⁸Ga-PSMA-11 PET/CT. However, the radiation exposure of these glands does play a role when using PSMA ligands for targeted radiotherapy. The first report about targeted radiotherapy of metastatic PCa with a PSMA-ligand has already described side effects such as dry mouth and mucositis [29].

Our analysis confirms that PCa metastases demonstrate an increase of PSMA ligand uptake over time [15, 19, 28–30]. We previously published that 70 % of PCa lesions have increased uptake and contrast at 3 h p.i. compared to 1 h p.i. [19]. However, as all representative 65 PCa lesions in the mentioned previous study were visible at 1 h p.i. with sufficient contrast, we recommended imaging at 1 h p.i. with later imaging only to clarify unclear findings. The 1-h time point allows easy integration of PSMA-11 PET/CT into the clinical

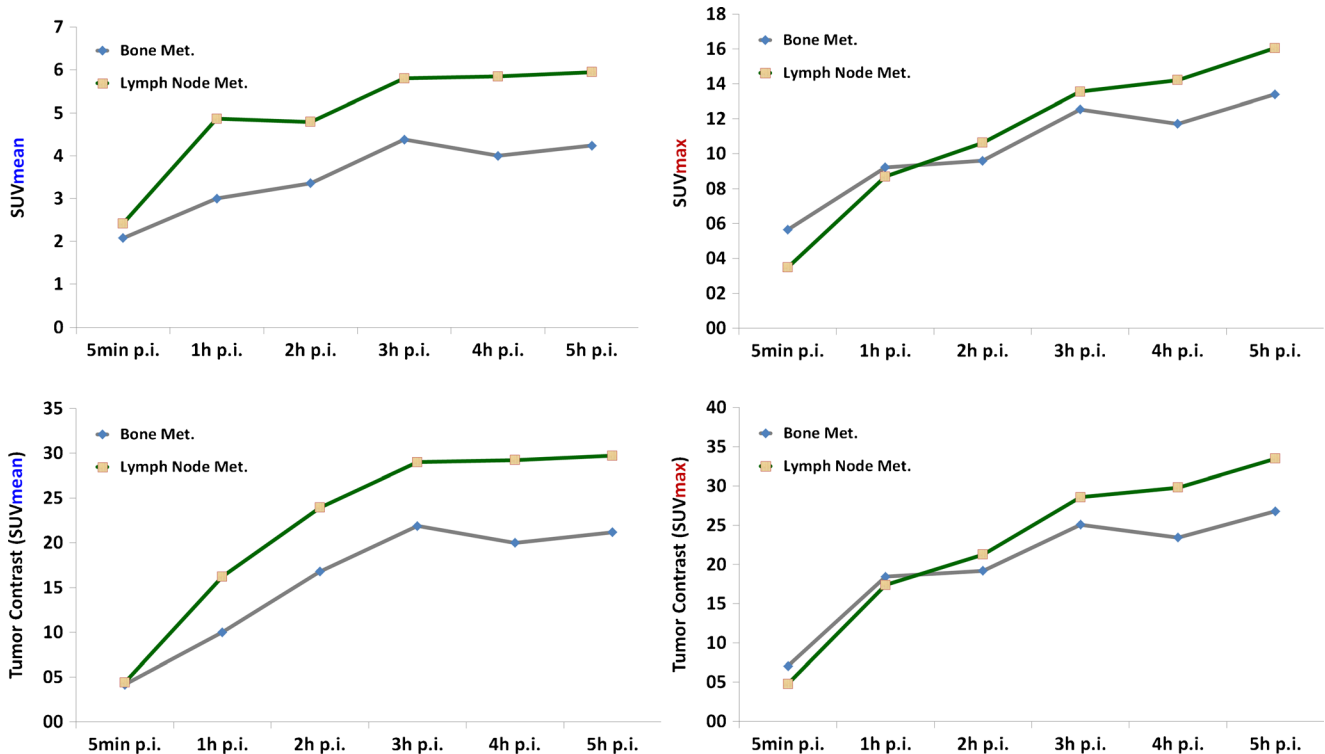


Fig. 5 Development of SUV values and tumor contrast over time in all PCa lesions detected in the patient group (five bone metastases and 11 LN metastases)

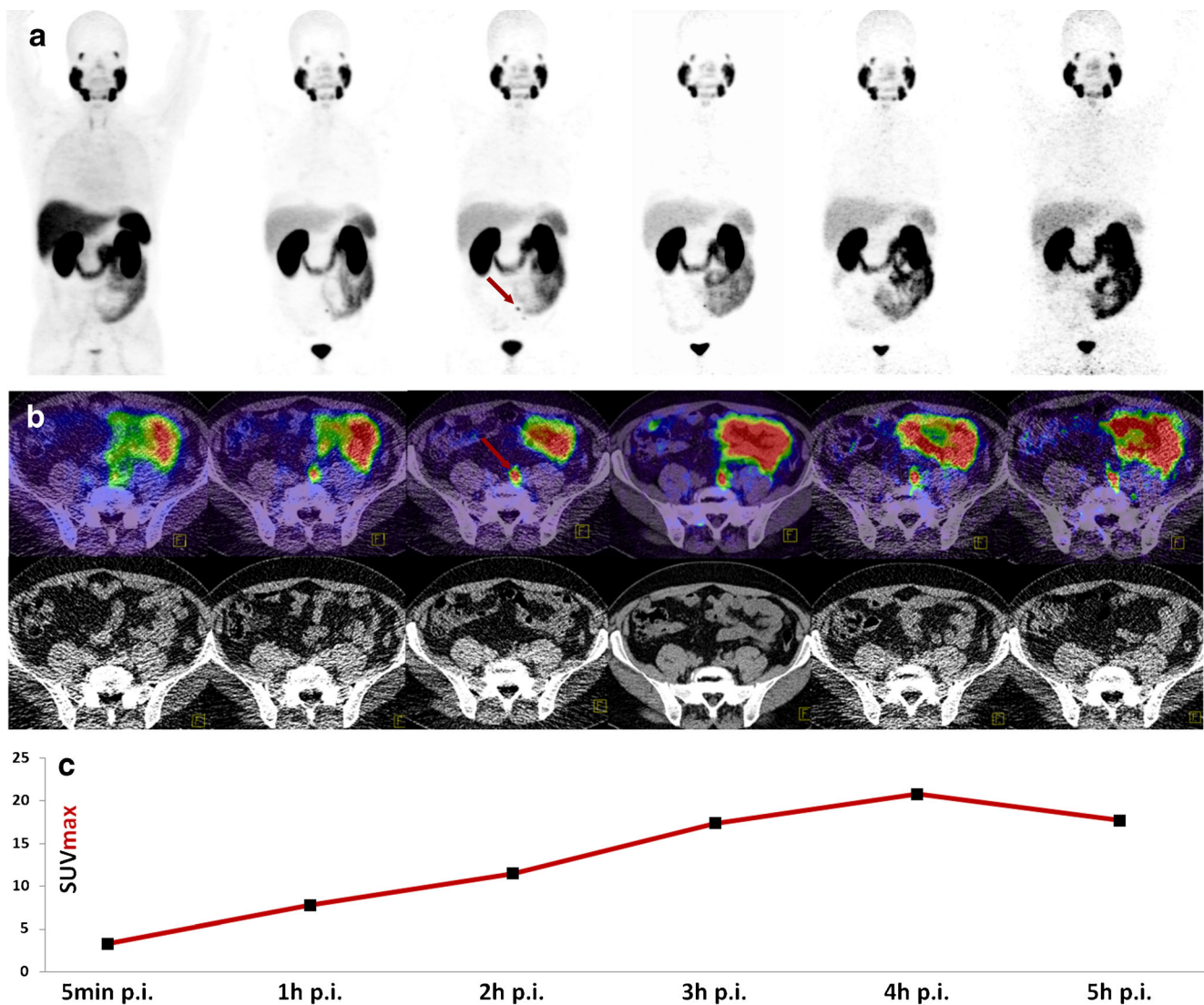


Fig. 6 Sequential PET/CT of patient no. 2 following the injection of 170 MBq ^{68}Ga -PSMA-11. Most prostate cancer lesions show an increase in uptake by time as shown by this figure. **a** Maximum

intensity projections (MIP) of the sequential PET/CT. **b** PET/CT fusion and $\text{CT}_{\text{low-dose}}$. **c** SUVmax of a lymph nodal metastasis (red arrows in **a** and **b**) at the different times

routine where multiple other PET scans are conducted at 1 h p.i. (^{18}F -FDG, ^{18}F -DOPA, ^{68}Ga -DOTATOC, etc.). In the present analysis however, six lesions in two different patients were not visible at 1 h p.i. due to low contrast, although these missed lesions did not change the tumor staging of the patients.

Overall, the question remains at what time following the injection of ^{68}Ga -PSMA-11 the PET-scans should be conducted. In this study, most PCa metastases were visible on PSMA PET conducted beyond 1 h p.i., with the best imaging time point being at 3 h p.i. Furthermore, we believe that these additionally detected lesions will rarely lead to a change of tumor stage or therapy procedure. Other clinical tracers (eg ^{18}F -FDG, ^{18}F -DOPA, ^{68}Ga -DOTATOC) are typically imaged at 1 h, and in this clinical workflow, imaging using multiple

scans and delayed imaging will require a complex planning. Conducting the ^{68}Ga -PSMA-11 PET/CT 1 h after tracer injection therefore would facilitate the planning of the clinical routine as well as increasing the patients comfort due to a shorter time of waiting. However, late images could be alternatively planned for patients with low PSA values to increase the probability of detecting tumor lesions.

One limitation of the current analysis is the lack of histopathological investigations of PET-positive lesions. However, since ^{68}Ga -PSMA-ligand PET/CT was introduced, the available data indicate that any uptake of PSMA-ligands above local background in CT-morphological visible lesions is highly specific for PCa and, thus, has to be regarded as PCa unless otherwise proven [21]. None of the lesions examined for this analysis were equivocal. A second limitation is the small

Table 4 SUVmean/max of all PCa lesions analyzed

SUVmean	5 min p.i.	1 h p.i.	2 h p.i.	3 h p.i.	4 h p.i.	5 h p.i.	SUVmax	5 min p.i.	1 h p.i.	2 h p.i.	3 h p.i.	4 h p.i.	5 h p.i.
Bone Met. 1	6.2	10	13.5	16	16.3	16.9	Bone Met. 1	20.1	37.5	41.2	48.6	48.51	53.1
Bone Met. 2	1.1	1.4	0.8	1.2	1.2	0.9	Bone Met. 2	1.6	2.7	1.9	5.5	3.3	3.7
Bone Met. 3	1.1	1	0.9	2.7	0.7	1.5	Bone Met. 3	3.8	1.8	1	3.4	2.1	5.6
Bone Met. 4	1.1	1.5	0.9	0.9	1.2	1.2	Bone Met. 4	1.6	2.7	2.6	3	3.3	3.4
Bone Met. 5	0.9	1.1	0.7	1.1	0.6	0.7	Bone Met. 5	1.1	1.4	1.3	2.2	1.4	1.2
LN Met. 1	3.5	9.7	9.5	9.6	12	11.6	LN Met. 1	4.9	11.9	12.6	14.6	17.3	20.3
LN Met. 2	3.4	7.5	6.9	7.8	7.3	7.3	LN Met. 2	4.8	9.5	11.5	10.6	12.8	18.8
LN Met. 3	4	7.2	6.1	10	7.6	7.7	LN Met. 3	4.9	12.4	13.2	26.9	19.7	22.9
LN Met. 4	2.2	4.7	3.3	4	4.6	6.2	LN Met. 4	3	6.9	5.6	4.9	8.5	16.9
LN Met. 5	2	2.4	2.4	3.5	2.7	1.9	LN Met. 5	2.3	3.2	3.2	4.9	3.9	3.1
LN Met. 6	2.7	10	7.8	8.7	10.5	11.1	LN Met. 6	4.5	22.4	27.6	29.7	39.4	40.2
LN Met. 7	2.3	4.2	7	8.2	7.8	7.4	LN Met. 7	5	15	22.9	25.2	24.7	24.5
LN Met. 8	1.7	1.6	2.5	2.5	2.4	1.7	LN Met. 8	2.1	2.5	4.6	6.7	4.9	3.9
LN Met. 9	2.4	3.3	4.1	4.6	6.9	5.9	LN Met. 9	3.3	7.8	11.5	17.4	20.8	17.7
LN Met. 10	1.3	1.4	1.7	1.8	0.8	1.6	LN Met. 10	1.8	2	2.4	3.5	1.5	3
LN Met. 11	1.1	1.5	1.4	3.1	1.7	3	LN Met. 11	1.5	2	1.9	4.7	2.9	5.3

Bold numbers indicate PCa lesions that were not sufficiently visible at specific times due to low contrast

number of patients, but the low standard deviation of the effective dose suggests that the analysis is representative for the radiation exposure of ^{68}Ga -PSMA-11 PET.

Conclusions

Physiological uptake of ^{68}Ga -PSMA-11 was observed in lacrimal and salivary glands, nasal mucosa, liver, spleen, kidneys, proximal small intestines, and in some parts of the large intestines. The kidneys were the organs receiving the highest absorbed dose. Additional organs with higher dose were urinary bladder, upper large intestines, and the spleen. The average effective dose with a highly sufficient diagnostic activity of 200 MBq is 4.7 mSv. Late images (e.g., at 3 h p.i.) show PCa metastases with improved tracer uptake and contrast compared to early images (e.g., at 1 h p.i.).

Acknowledgments We express our gratitude to the Klaus Tschira Foundation (grant no. 00.198.2012) for funding our research. In addition, we would like to thank our staff, in particular Stephanie Biedenstein, Kirsten Kunze, Larissa Engel, and Peter Seybold for their help in performing this analysis.

Compliance with ethical standards

Funding This study was funded by the Klaus Tschira Foundation (grant no. 00.198.2012).

Conflict of interest Ali Afshar-Oromieh has received honoraria from Siemens Healthcare for one educational talk. All other authors declare that they have no conflict of interest.

Ethical approval All patients published in this manuscript signed a written informed consent form for the purpose of anonymized evaluation and publication of their data. All reported investigations were conducted in accordance with the Helsinki Declaration and with our national regulations (German Medicinal Products Act, AMG §13 2b). This evaluation was approved by the ethics committee of the University of Heidelberg (S-321-2012).

References

1. Siegel R, Ma J, Zou Z, Jemal A. Cancer statistics. *CA Cancer J Clin.* 2014;64:9–29.
2. Schmid DT, John H, Zweifel R, Cservenyak T, Westera G, Goerres GW, et al. Fluorocholine PET/CT in patients with prostate cancer: initial experience. *Radiology.* 2005;235:623–8.
3. Igerc I, Kohlfurst S, Gallowitsch HJ, Matschnig S, Kresnik E, Gomez-Segovia I, et al. The value of 18F-choline PET/CT in patients with elevated PSA-level and negative prostate needle biopsy for localisation of prostate cancer. *Eur J Nucl Med Mol Imaging.* 2008;35:976–83.
4. Kwee SA, DeGrado T. Prostate biopsy guided by 18F-fluorocholine PET in men with persistently elevated PSA levels. *Eur J Nucl Med Mol Imaging.* 2008;35:1567–9. author reply 1570.
5. Hacker A, Jeschke S, Leeb K, Prammer K, Ziegerhofer J, Segal W, et al. Detection of pelvic lymph node metastases in patients with clinically localized prostate cancer: comparison of [18F]fluorocholine positron emission tomography-computerized tomography and laparoscopic radioisotope guided sentinel lymph node dissection. *J Urol.* 2006;176:2014–8–9.
6. Sweat SD, Pacelli A, Murphy GP, Bostwick DG. Prostate-specific membrane antigen expression is greatest in prostate adenocarcinoma and lymph node metastases. *Urology.* 1998;52:637–40.

7. Mannweiler S, Amersdorfer P, Trajanoski S, Terrett JA, King D, Mehes G. Heterogeneity of prostate-specific membrane antigen (PSMA) expression in prostate carcinoma with distant metastasis. *Pathol Oncol Res.* 2009;15:167–72.
8. Hillier SM, Maresca KP, Femia FJ, Marquis JC, Foss CA, Nguyen N, et al. Preclinical evaluation of novel glutamate-urea-lysine analogues that target prostate-specific membrane antigen as molecular imaging pharmaceuticals for prostate cancer. *Cancer Res.* 2009;69:6932–40.
9. Maresca KP, Hillier SM, Femia FJ, Keith D, Barone C, Joyal JL, et al. A series of halogenated heterodimeric inhibitors of prostate specific membrane antigen (PSMA) as radiolabeled probes for targeting prostate cancer. *J Med Chem.* 2009;52:347–57.
10. Cho SY, Gage KL, Mease RC, Senthambichelvan S, Holt DP, Jeffrey-Kwanisai A, et al. Biodistribution, tumor detection, and radiation dosimetry of 18F-DCFBC, a low-molecular-weight inhibitor of prostate-specific membrane antigen, in patients with metastatic prostate cancer. *J Nucl Med Off Publ Soc Nucl Med.* 2012;53:1883–91.
11. Barrett JA, Coleman RE, Goldsmith SJ, Vallabhajosula S, Petry NA, Cho S, et al. First-in-man evaluation of 2 high-affinity PSMA-avid small molecules for imaging prostate cancer. *J Nucl Med Off Publ Soc Nucl Med.* 2013;54:380–7.
12. Tagawa ST, Milowsky MI, Morris M, Vallabhajosula S, Christos P, Akhtar NH, et al. Phase II study of Lutetium-177-labeled anti-prostate-specific membrane antigen monoclonal antibody J591 for metastatic castration-resistant prostate cancer. *Clin Cancer Res Off J Am Assoc Cancer Res.* 2013;19:5182–91.
13. Hillier SM, Maresca KP, Lu G, Merkin RD, Marquis JC, Zimmerman CN, et al. 99mTc-labeled small-molecule inhibitors of prostate-specific membrane antigen for molecular imaging of prostate cancer. *J Nucl Med Off Publ Soc Nucl Med.* 2013;54:1369–76.
14. Banerjee SR, Pullambhatla M, Foss CA, Nimmagadda S, Ferdani R, Anderson CJ, et al. ⁶⁴Cu-labeled inhibitors of prostate-specific membrane antigen for PET imaging of prostate cancer. *J Med Chem.* 2014;57:2657–69.
15. Szabo Z, Mena E, Rowe SP, Plyku D, Nidal R, Eisenberger MA, et al. Initial evaluation of [(18)F]DCFPyL for prostate-specific membrane antigen (PSMA)-targeted PET imaging of prostate cancer. *Mol Imaging Biol MIB Off Publ Acad Mol Imaging.* 2015;17:565–74.
16. Schäfer M, Bauder-Wüst U, Leotta K, Zoller F, Mier W, Haberkorn U, et al. A dimerized urea-based inhibitor of the prostate-specific membrane antigen for 68Ga-PET imaging of prostate cancer. *EJNMMI Res.* 2012;2:23.
17. Eder M, Schäfer M, Bauder-Wüst U, Hull W-E, Wängler C, Mier W, et al. 68Ga-complex lipophilicity and the targeting property of a urea-based PSMA inhibitor for PET imaging. *Bioconjug Chem.* 2012;23:688–97.
18. Afshar-Oromieh A, Haberkorn U, Eder M, Eisenhut M, Zechmann CM. [68Ga]Gallium-labelled PSMA ligand as superior PET tracer for the diagnosis of prostate cancer: comparison with 18F-FECH. *Eur J Nucl Med Mol Imaging.* 2012;39:1085–6.
19. Afshar-Oromieh A, Malcher A, Eder M, Eisenhut M, Linhart HG, Hadaschik BA, et al. PET imaging with a [68Ga]gallium-labelled PSMA ligand for the diagnosis of prostate cancer: biodistribution in humans and first evaluation of tumour lesions. *Eur J Nucl Med Mol Imaging.* 2013;40:486–95.
20. Afshar-Oromieh A, Zechmann CM, Malcher A, Eder M, Eisenhut M, Linhart HG, et al. Comparison of PET imaging with a (68)Ga-labelled PSMA ligand and (18)F-choline-based PET/CT for the diagnosis of recurrent prostate cancer. *Eur J Nucl Med Mol Imaging.* 2014;41:11–20.
21. Afshar-Oromieh A, Avtzi E, Giesel FL, Holland-Letz T, Linhart HG, Eder M, et al. The diagnostic value of PET/CT imaging with the (68)Ga-labelled PSMA ligand HBED-CC in the diagnosis of recurrent prostate cancer. *Eur J Nucl Med Mol Imaging.* 2015;42:197–209.
22. Eiber M, Maurer T, Souvatzoglou M, Beer AJ, Ruffani A, Haller B, et al. Evaluation of hybrid ⁶⁸Ga-PSMA ligand PET/CT in 248 patients with biochemical recurrence after radical prostatectomy. *J Nucl Med Off Publ Soc Nucl Med.* 2015;56:668–74.
23. Eder M, Neels O, Müller M, Bauder-Wüst U, Remde Y, Schäfer M, et al. Novel preclinical and radiopharmaceutical aspects of [68Ga]Ga-PSMA-HBED-CC: a new PET tracer for imaging of prostate cancer. *Pharm Basel Switz.* 2014;7:779–96.
24. Reza Ay M, Zaidi H. Computed tomography-based attenuation correction in neurological positron emission tomography: evaluation of the effect of the X-ray tube voltage on quantitative analysis. *Nucl Med Commun.* 2006;27:339–46.
25. Stabin MG, Sparks RB, Crowe E. OLINDA/EXM: the second-generation personal computer software for internal dose assessment in nuclear medicine. *J Nucl Med.* 2005;46:1023–7.
26. 1990 Recommendations of the International Commission on Radiological Protection. *Ann ICRP.* 1991;21:1–201.
27. Krohn T, Verburg FA, Pufe T, Neuhuber W, Vogg A, Heinzel A, et al. [Ga]PSMA-HBED uptake mimicking lymph node metastasis in coeliac ganglia: an important pitfall in clinical practice. *Eur J Nucl Med Mol Imaging* [Internet]. Available from: http://www.ncbi.nlm.nih.gov/entrez/query.fcgi?cmd=Retrieve&db=PubMed&dopt=Citation&list_uids=25248644.
28. Herrmann K, Bluemel C, Weineisen M, Schottelius M, Wester H-J, Czernin J, et al. Biodistribution and radiation dosimetry for a probe targeting prostate-specific membrane antigen for imaging and therapy. *J Nucl Med Off Publ Soc Nucl Med.* 2015;56:855–61.
29. Zechmann CM, Afshar-Oromieh A, Armor T, Stubbs JB, Mier W, Hadaschik B, et al. Radiation dosimetry and first therapy results with a (124)I/ (131)I-labeled small molecule (MIP-1095) targeting PSMA for prostate cancer therapy. *Eur J Nucl Med Mol Imaging.* 2014;41:1280–92.
30. Afshar-Oromieh A, Hetzheim H, Kratochwil C, Benesova M, Eder M, Neels OC, et al. The Theranostic PSMA ligand PSMA-617 in the diagnosis of prostate cancer by PET/CT: biodistribution in humans, radiation dosimetry, and first evaluation of tumor lesions. *J Nucl Med Off Publ Soc Nucl Med.* 2015;56:1697–705.

European Journal of Nuclear Medicine & Molecular Imaging is a copyright of Springer, 2016.
All Rights Reserved.